Turkish Journal of Earth Sciences (Turkish J. Earth Sci.), Vol. 20, 2011, pp. 411–427. Copyright ©TÜBİTAK
doi:10.3906/yer-0910-48 First published online 14 June 2010

Palaeoearthquakes on the Kelkit Valley Segment of the North Anatolian Fault, Turkey: Implications for the Surface Rupture of the Historical 17 August 1668 Anatolian Earthquake

CENGİZ ZABCI[1,*], HÜSNÜ SERDAR AKYÜZ[1], VOLKAN KARABACAK[2], TAYLAN SANÇAR[3,4], ERHAN ALTUNEL[2], HALİL GÜRSOY[5] & ORHAN TATAR[5]

[1] İstanbul Teknik Üniversitesi, Ayazağa Yerleşkesi, Jeoloji Mühendisliği Bölümü, Maslak, TR–34469 İstanbul, Turkey (E-mail: zabci@itu.edu.tr)
[2] Eskişehir Osmangazi Üniversitesi, Jeoloji Mühendisliği Bölümü, TR–26040 Eskişehir, Turkey
[3] İstanbul Teknik Üniversitesi, Ayazağa Yerleşkesi, Avrasya Yerbilimleri Enstitüsü, Maslak, TR–34469 İstanbul, Turkey
[4] Tunceli Üniversitesi, Mühendislik Fakültesi, Jeoloji Mühendisliği Bölümü, TR–62000 Tunceli, Turkey
[5] Cumhuriyet Üniversitesi, Jeoloji Mühendisliği Bölümü, TR–58140 Sivas, Turkey

Received 02 November 2009; revised typescript receipts 20 May 2010; accepted 14 June 2010

Abstract: The 26 December 1939 Erzincan (M_s= 7.8) and 20 December 1942 Erbaa-Niksar (M_s= 7.1) earthquakes created a total surface rupture more than 400 km between Erzincan and Erbaa on the middle to eastern sections of the North Anatolian Fault. These two faulting events are separated by a 10-km-wide releasing stepover, which acted like a seismic barrier in the 20th century. To understand the rupture behaviour in this structurally complex section of the North Anatolian Fault, we undertook palaeoseismological trench investigations on the Kelkit Valley segment where there is little or no palaeoseismic information. We found evidence for three surface faulting earthquakes predating the 1939 event during the past millennium in trenches excavated in Reşadiye and Umurca. In addition to the 1939 Erzincan earthquake, prior surface ruptures are attributed to the 17 August 1668, A.D. 1254 and A.D. 1045 events. Surface rupture of the 17 August 1668 Anatolian earthquake was previously reported in palaeoseismological studies, performed on the 1944, 1943, and 1942 earthquake fault segments. We suggest that the surface rupture of this catastrophic event jumped the 10-km-wide releasing stepover in Niksar and continued eastward to near Koyulhisar. The existence of different amount of offsets in field boundaries (sets of 4 m, 6.5 m, and 10.8 m) was interpreted as the result of multiple events, in which the 1939, 1668, and 1254 surface ruptures have about 4, 2.5, and 4 metres of horizontal coseismic slip on the Kelkit Valley segment of the North Anatolian Fault, respectively.

Key Words: North Anatolian Fault, palaeoseismicity, earthquakes, Kelkit Valley, Turkey, 1668 Anatolian earthquake

Kuzey Anadolu Fayı, Kelkit Vadisi Segmenti'nin Eski Depremleri: Tarihsel 17 Ağustos 1668 Anadolu Depreminin Yüzey Kırığı ile İlgili Bulgular

Özet: Kuzey Anadolu Fayı'nın orta ve doğu kesimlerinde gerçekleşen 26 Aralık 1939 Erzincan (M_s= 7.8) ve 20 Aralık 1942 Erbaa-Niksar (M_s= 7.1) depremleri, Erzincan ve Erbaa arasında toplam 400 km'den daha uzun bir yüzey kırığı yaratmıştır. Bu iki faylanma olayı, 20. yüzyılda sismik bir bariyer işlevi görmüş olan 10 km genişliğindeki açılmalı bir sıçrama ile birbirlerinden ayrılır. Kuzey Anadolu Fayı'nın yapısal olarak karmaşık bu kısımının sahip olduğu kırılma davranışının daha iyi anlaşılması için Kelkit Vadisi segmenti üzerinde paleosismolojik hendek çalışmaları gerçekleştirilmiştir. Reşadiye ve Umurca'da açılan iki hendek sonucu son bin yıl içerisinde gerçekleşmiş 1939 Erzincan depremine ek olarak toplam üç olay tespit edilmiştir. Bunlar, sırasıyla 17 Ağustos 1668, M.S. 1254 ve M.S. 1045 tarihsel depremleri ile deneştirilmişlerdir. 17 Ağustos 1668 Anadolu depremine ait yüzey kırığı, 1942, 1943 ve 1944 deprem fay segmentlerinin üzerinde daha önceden gerçekleştirilen birçok paleosismoloji çalışmasında belirlenmiştir. Bu büyük deprem, Kelkit Vadisi segmenti üzerinde açılan hendeklerin sonuçlarına göre, Niksar'da yer alan 10 km genişlikteki açılmalı sıçramayı aşmış ve Koyulhisar yakınlarına kadar uzanan bir alana kadar kırılmıştır. Ayrıca, tarla sınırları üzerinde ölçülen farklı ötelenme miktarlarının (4, 6.5 ve 10.8 m) varlığı, birden fazla depremin etkisi olarak yorumlanmıştır. Buna göre Kuzey Anadolu Fayı, Kelkit Vadisi segmenti üzerinde, yaklaşık 4 m'lik atım 1939 Erzincan, 2.5 m'lik atım 1668, 4 m'lik atım 1254 depremleri sonucunda gerçekleşmiş olmalıdır.

Anahtar Sözcükler: Kuzey Anadolu Fayı, paleosismisite, depremler, Kelkit Vadisi, Türkiye, 1668 Anadolu depremi

Introduction

The North Anatolian Fault (NAF) is one of the world's most important active dextral strike-slip structures, extending more than 1500 km from eastern Turkey to the northern Aegean Sea (Figure 1a). This deformation zone is the northern boundary of the westward moving Anatolian block and connects the Aegean extensional regime with East Anatolian high plateau (Ketin 1948; Şengör 1979; Barka & Kadinsky-Cade 1988; Barka 1992; Şengör *et al.* 2005). Eight large earthquakes occurred along the NAFZ between 1939 and 1999, in a westward-migrating sequence, along a 1000-km-long zone of continuous surface ruptures (Blumenthal 1945; Ambraseys & Zatopek 1969; Ketin 1969; Barka 1996, 1999; Akyüz *et al.* 2002; Barka *et al.* 2002; Kondo *et al.* 2005; Pucci *et al.* 2006).

The 26 December 1939 Erzincan (M_s = 7.8) and 20 December 1942 Erbaa-Niksar (M_s = 7.1) earthquakes created a total surface rupture more than 400 km between Erzincan and Erbaa (Figure 1b) (Ketin 1969; Barka 1996; Ambraseys & Jackson 1998). As

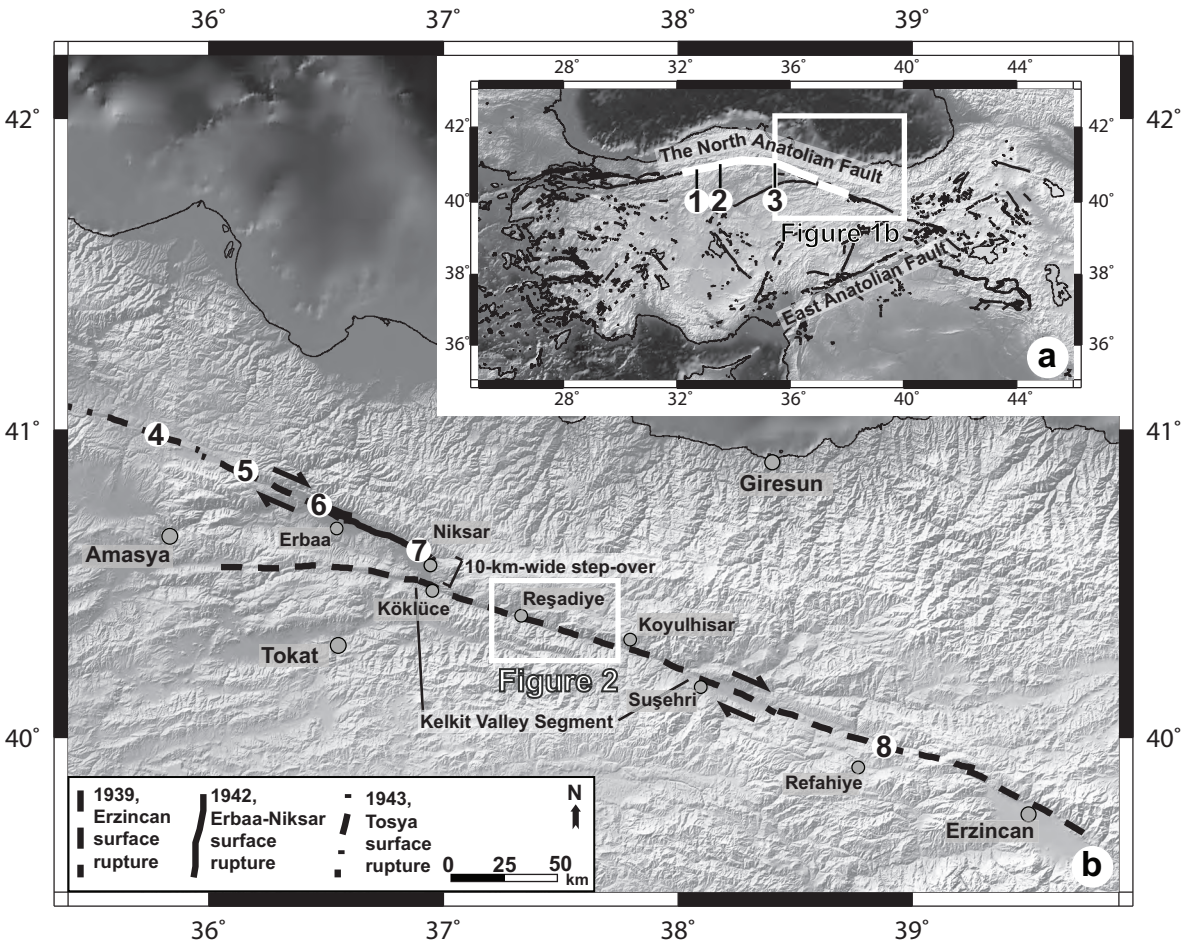

Figure 1. **(a)** Map of the North Anatolian Fault and other active faults in Turkey (Şaroğlu *et al.* 1992). Numbers indicate palaeoseismic trench sites, 1– Okumura *et al.* (2003) & Kondo *et al.* (2004, 2010), 2– Sugai *et al.* (1999), 3– Yoshioka *et al.* (2000). White lines show the location and probable extent of faulting associated with the earthquake of 1668. **(b)** Simplified map shows traces of 1939, 1942 and partly 1943 earthquake ruptures (drawn from Ketin 1969 and Barka 1996). The 10-km-wide releasing stepover is clearly visible between 1939 and 1942 ruptures, extending between Niksar and Köklüce. Numbered circles are locations of previous trenches performed by 4– Hartleb *et al.* (2003), 5– Fraser *et al.* (2009), 6– Kurçer *et al.* (2009), 7– Kondo *et al.* (2009) and 8– Hartleb *et al.* (2006).

Figure 1b shows, these two earthquake segments are separated by a 10-km-wide releasing stepover, near Köklüce, at the eastern boundary of the Niksar Basin (Barka & Kadinsky-Cade 1988; Barka *et al.* 2000). This geometric discontinuity of the fault zone acts as a seismic barrier, stopping rupture propagation or changing its direction in the 1939 and 1942 ruptures (Wesnousky 1988). In contrast, the historical Anatolian Earthquake of 17 August 1668, thought to have a probable rupture length of more than 400 km, starts from east of Gerede, crossing the 10-km-wide releasing stepover in Niksar, and terminates near Koyulhisar (Figure 1a) (Ambraseys & Finkel 1988). However, some other historical earthquake catalogues (e.g., Pınar & Lahn 1952; Ergin *et al.* 1967) suggest that instead of one large earthquake, a series of events occurred between July and September 1668 in various places (Pınar & Lahn 1952; Ergin *et al.* 1967). Because of ambiguity in the historical information, the spatial distribution of the 1668 rupture and recurrence of large prior earthquakes in this region can only be derived from palaeoseismology. Several palaeoseismological investigations were carried out in the west of the 10-km-wide releasing stepover (Figure 1b) (Sugai *et al.* 1999; Yoshioka *et al.* 2000; Hartleb *et al.* 2003; Okumura *et al.* 2003; Kondo *et al.* 2004, 2009; Fraser *et al.* 2009; Kurçer *et al.* 2009). The Ardıçlı trench site (located 9 km east of Gerede) and the Demirtepe trench site (located 12 km east of Gerede) expose the penultimate event in A.D. 1668 (Okumura *et al.* 2003; Kondo *et al.* 2004, 2010). This location is the westernmost evidence for the extent of the 1668 rupture determined by palaeoseismological studies. These data are in agreement with the Ardıçlı trench site, 3 km east of Kondo *et al.* (2004) and Kondo *et al.* (2010)'s study area (site 1 in Figure 1a) (Okumura *et al.* 2003). Further east, one event prior to the 1943 rupture is dated to between A.D. 1495–1850 in the Ilgaz-Aluc trench site (site 2 in Figure 1a) and is correlated with the A.D. 1668 historical earthquake (Sugai *et al.* 1999). Hartleb *et al.* (2003) also interpreted the penultimate event in the Alayurt trenches (site 4 in Figure 1b) with this large historical event. In a recent study, Fraser *et al.* (2009) correlated the penultimate event to probably A.D. 1668 or possibly to A.D. 1598 from the results of their trench study at Destek (site 5 in Figure 1b). However, the surface faulting of the 17 August 1668 earthquake is not reported in the Havza trenches (site 3 in Figure 1a) (Yoshioka *et al.* 2000). Signs of the 1668 historical event are documented by Kurçer *et al.* (2009) (site 6 in Figure 1b) and Kondo *et al.* (2009) (site 7 in Figure 1b) on the most western and eastern sections of the 1942 Erbaa-Niksar rupture as the most eastern evidence for faulting during the 1668 event. Although palaeoseismic evidence exists for the rupture of the 1668 earthquake on 1942, 1943 and 1944 ruptures, there are no signs of a historical earthquake between the 14th and 19th century on the 1939 Erzincan earthquake surface rupture. At the Çukurçimen site (site 8 in Figure 1b) evidence for faulting prior to the 1939 event has an upper age limit of A.D. 1420 and is interpreted to be the A.D. 1254 historical earthquake (Hartleb *et al.* 2006). This information suggests that surface rupture of the 1668 earthquake did not extent further east than Refahiye.

In the light of the above discussion, the main objective of this study is to provide more constraints to evaluate the 17 August 1668 Anatolian earthquake rupture distribution. It is very important to understand the following questions; does a releasing stepover, with a width of 10 km, act as a seismic-barrier like it did on 1939 and 1942 earthquakes, or can it be crossed by a surface rupture produced by the release of very high seismic energy? Any evidence about the rupture process on this complex fault geometry will give us a better understanding for the construction of more realistic seismic hazard analysis. We excavated two palaeoseismic trenches (Figure 1b) on the Kelkit Valley segment of the 1939 rupture, where we tried to find evidence of any palaeoevents, as close as possible to this seismic barrier (the releasing stepover).

26 December 1939 Erzincan Earthquake: Kelkit Valley Segment

The Erzincan earthquake of 26 December 1939 was a large (Ms 7.8) event (Ambraseys & Jackson 1998), which created a rupture zone about 360 km long, extended from the eastern end of the Erzincan Basin to south of Amasya (Figure 1b) (Barka 1996). The epicentre is approximately 10 km NW of Erzincan (39.80°N, 39.38°E) (Dewey 1976). The focal mechanism defines a fault plane striking 108° and dipping at 86°, with almost pure strike-slip motion (McKenzie 1972).

The 1939 rupture consists of five major geometric segments: (a) the Erzincan segment, (b) The Mihar-Tümekar segment, (c) the Ortaköy-Suşehri segment, (d) the Kelkit Valley segment, and (e) Ezinepazarı segment (Barka 1996). The Kelkit Valley segment is approximately 100 km long and deviates from the Ortaköy-Suşehri and Ezinepazarı segments by bending of the fault zone to the east and west, respectively. Moreover, a 10-km-wide releasing stepover separates this section of the fault from the 1942 rupture (Barka *et al.* 2000). An average right-lateral slip of 7 m on the Ortaköy-Suşehri and Mihar-Tümekar segments decreases to an average value of 4 m on the Kelkit Valley segment. A 3.7 m dextral displacement of a road with a line of trees at Reşadiye (Parejas *et al.* 1942) was measured, just after the earthquake, approximately 200 km west of the epicentre. Barka (1996) added more measurements, which change from 4.5 m at Koyulhisar in the east, to 3.4 m at Köklüce in the west for the same segment. We have extended coseismic slip measurements at various locations of the Kelkit Valley segment. These additional measurements and the slip data from previous studies, expressing the coseismic slip distribution of the 1939 rupture on the Kelkit Valley segment, are compiled in Table 1. The collected data show a uniform coseismic slip of about 4 m after the 1939 earthquake on this section of the fault zone.

Paleoseismic Trenching on the Kelkit Valley Segment

We excavated 3 trenches at two different sites near Reşadiye and Umurca, along the Kelkit Valley

Table 1. Slip measurements along the Kelkit Valley segment of the 1939 Erzincan earthquake rupture zone. A, B, C and D indicate reliability of measurements (very good, good, fair and not clear, respectively) according to the method of measurement (tape measure, total station...etc) and the clearness of offset features (wall, road, fence, field boundary...etc).

Site	Site name	Lon (wgs84)	Lat (wgs84)	Offset feature	Horizontal offset	Quality	Villager confirm.	Notes
1	Ormancık	36.9078	40.5068	field boundary	3.9±0.8 m	C	–	this study
2	Camidere	36.9612	40.4915	field boundary	3.8±0.8 m	C	–	this study
3	Köklüce			wall	3-3.5 m			by Parejas et al (1942)
4	Köklüce			road	3.4 m	B	+	by Barka (1996)
5	Köklüce	36.9923	40.477	field boundary	3.9±0.8 m	C	–	this study
6	Reşadiye			road and line of trees	3.7 m			by Parejas et al (1942)
7	Reşadiye	37.3583	40.3835	field boundary	4.1±0.3 m	B	+	this study
8	Reşadiye	37.3586	40.3834	field boundary	4.3±0.4 m	B	+	this study
9	W of Umurca	37.5213	40.3413	field boundary	3.9±0.8 m	B	–	this study
10	Gökdere	37.6247	40.3174	field boundary	4.1±0.8 m	B	–	this study
11	Gökdere	37.6411	40.3133	field boundary	3.8±0.8 m	C	–	this study
12	Yeşilyurt	37.6917	40.299	field boundary	4.5±1.0 m	C	–	this study
13	Çaylı			irrigation canal	4.5 m	B	+	by Barka (1996)
14	Çimenli	37.7355	40.2918	field boundary	4.3±0.6 m	D	–	this study

segment of the 1939 surface rupture (Figure 2). Trench site selection was chosen on late Holocene alluvial sediments, where the 1939 rupture is confirmed by villagers or there is a clear sign of individual or cumulative coseismic slip offset nearby. Collected samples were dated by Accelerator Mass Spectrometry (AMS) and all ^{14}C dated samples are calibrated by OxCal version 4.1.3 (Bronk Ramsey 2009), in which atmospheric correction curves are those of Reimer *et al.* (2004) (Table 2).

In the following section, we report only two trenches, because dating results show a lack of continuous sedimentation or sampling of reworked, very small datable material in one of the trenches in the Reşadiye site, where evidence of several branches of faulting and three palaeoevents including the 1939 rupture were logged. We discuss the observations and interpretations of structural features of each trench site from west to east.

Reşadiye Trench

The Reşadiye trench was excavated in alluvial fan deposits perpendicular to the trace of the fault zone about 2 km east of Reşadiye town (RSD site in Figures 2 & 3a). In this area, approximately 4 m dextral offsets of the 1939 rupture are recorded at several field boundaries (Table 1, Figure 3a). Two field boundaries are horizontally offset by about 6.5 m and 10.5 m in the same location and this difference probably resulted from multiple events at this site (Figure 3a, b).

The trench is about 12 m long and 2.5 m deep, exposing a sequence of predominantly fine- to

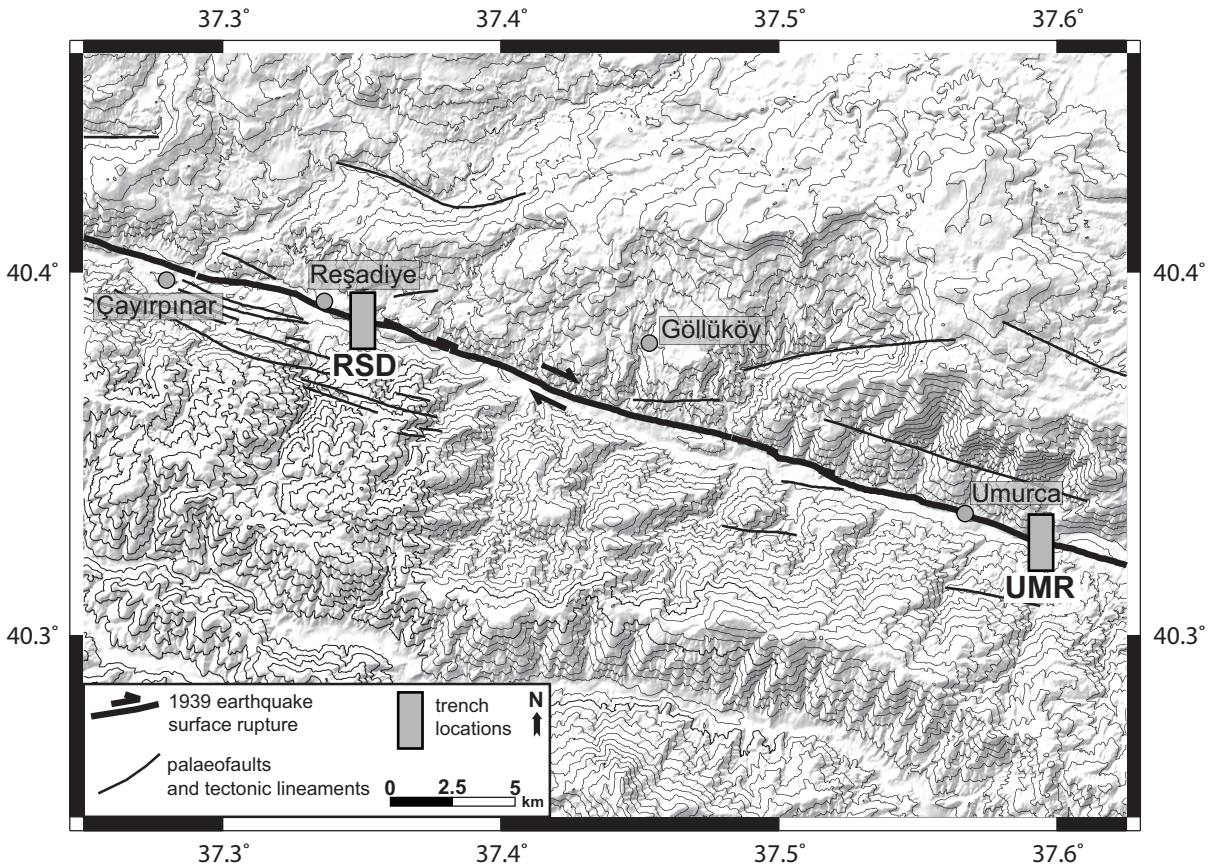

Figure 2. Simplified map shows trace of the 1939 surface rupture, some probable palaeotectonic faults and tectonic lineaments (compiled from Ketin 1969; Seymen 1975; Barka 1996). Trench sites are shown by rectangles (RSD– Reşadiye site; UMR– Umurca site).

Table 2. Measured and calibrated radiocarbon ages of samples collected from the Reşadiye and Umurca trenches. Measurements are calibrated by OxCal version 4.1.3 (Bronk Ramsey 2009) in which atmospheric correction curves are those by Reimer *et al.* (2004).

Lab	Sample	Radiocarbon age B.P.	$\delta^{13}C$	Calibration	Probability 0.95 (2σ)	Type of material
AA78143	R2-02	974±34	-24	A.D. 998–1004	1.20%	charcoal
				A.D. 1013–1157	94.20%	
AA78144	R2-04	1037±41	–23.4	A.D. 893–1045	91.30%	charcoal
				A.D. 1095–1120	3.30%	
				A.D. 1141–1148	0.80%	
AA78145	R2-07	937±34	–22.6	A.D. 1021–1172	95.40%	charcoal
AA78146	R2-11	3539±52	–6.2	B.C. 2024–1742	95.40%	charcoal
AA78147	R2-14	417±37	–25	A.D. 1423–1523	79.70%	charcoal
				A.D. 1574–1626	15.70%	
KIA31198	UMR B-1	4180±35	–22.79±0.19	B.C. 2889–2833	22.00%	charcoal
				B.C. 2819–2662	71.10%	
				B.C. 2650–2635	2.30%	
KIA31200	UMR B-3	1790±100	–28.51±0.22	A.D. 2–436	94.10%	charcoal
				A.D. 490–510	0.80%	
				A.D. 517–529	0.50%	
KIA31201	UMR B-4	270±25	–25.38±0.12	A.D. 1521–1577	35.30%	charcoal
				A.D. 1582–1591	1.70%	
				A.D. 1622–1668	53.70%	
				A.D. 1782–1797	4.70%	
KIA31202	UMR B-9	1035±50	–23.90±0.20	A.D. 890–1052	84.00%	charcoal
				A.D. 1081–1128	8.60%	
				A.D. 1135–1153	2.90%	
AA78138	UMR B-7	1534±36	–24.3	A.D. 430–600	95.40%	charcoal
KIA31204	UMR D-1	185±30	–22.38±0.12	A.D. 1650–1695	20.80%	charcoal
				A.D. 1726–1814	53.30%	
				A.D. 1838–1842	0.40%	
				A.D. 1853–1867	1.30%	
				A.D. 1874–1875	0.09%	
				A.D. 1918–1955	19.60%	
KIA31205	UMR D-2	470±25	–22.18±0.16	A.D. 1415–1451	95.40%	charcoal

medium-grained clastic sediments (clay, silt, and sand), with intercalated layers of pebbles (Figure 4). Pebbles and cobbles are exposed at the bottom, along the trench wall. A description of all stratigraphic units is given in Figure 4. Five charcoal samples were dated by AMS from units b, d, g, j, and m (samples R2-02, R2-04, R2-07, R2-11, R2-14 see Table 2 and Figure 4). While a single reworked sample is dated to be B.C. 2024–1742, others yield ages ranging from A.D. 1423–1523 to A.D. 893–1045.

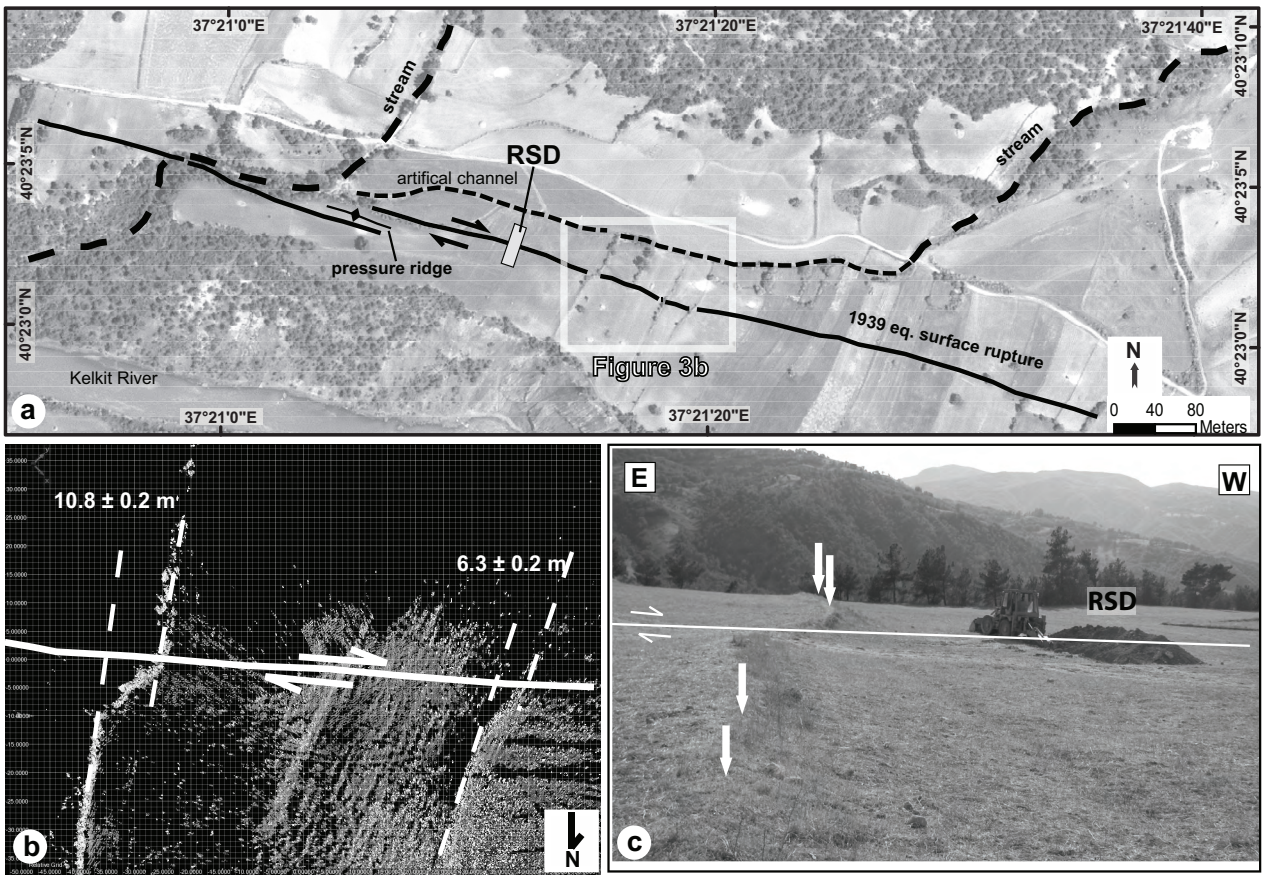

Figure 3. **(a)** Ikonos satellite image shows offset features and trace of the 1939 surface rupture in the Reşadiye trench site (RSD). An artificial channel modifies the sedimentation and drains the eastern channel by diverting it to the western drainage system. Note dextral offset in white rectangle. **(b)** The point cloud data of the Terrestrial LIDAR survey of different magnitude field boundary offsets (location is shown in Figure 3a). Two different offsets (10.8±0.2 m and 6.3±0.2 m) are measured on two different field boundaries along the 1939 surface rupture. **(c)** Close up view of the Reşadiye trench site. White arrows show the offset field boundary.

On the western wall of the trench (Figure 4) is exposed a single fault zone, comprising multiple strands between the first and fifth metres of the trench wall. Two sub-parallel fault branches F2 and F3 reach up to the ploughed zone as the result of 1939 rupture at the fourth metre. However, the southernmost single branch (F1) was not activated in the 1939 earthquake and terminates about 0.5 m below the recent surface.

The ploughed soil is thickened at the fourth metre due to local subsidence during the 1939 event (RSD-1). There is a clear downthrow to the north along the 1939 rupture (faults F2 – F3): the northern side (units e, g and l) is downthrown by up to 25 cm (Figure 4). Unit c is the post seismic infill material composed of clay material with coarse pebbles and cobbles probably thrown by local people into the fissures and cracks which opened during the 1939 coseismic surface rupture. Some stratigraphic units (h, d, j, and k) show lateral discontinuities on each side of the fault branches F2 and F3.

Fault F1 cuts units m-g, with the northern side downthrown by up to 25 cm along the fault (Figure 4). We interpreted this truncation below unit f as evidence of the penultimate event (RSD-2) in the Reşadiye trench. Deformed strata are unconformably overlain by folded units f and e. Unit b is deposited across the north-facing scarp of F1, thus it thickens in the downthrown side (Figure 4). The event horizon for RSD-2 is the bottom of unit f. Of 4 samples

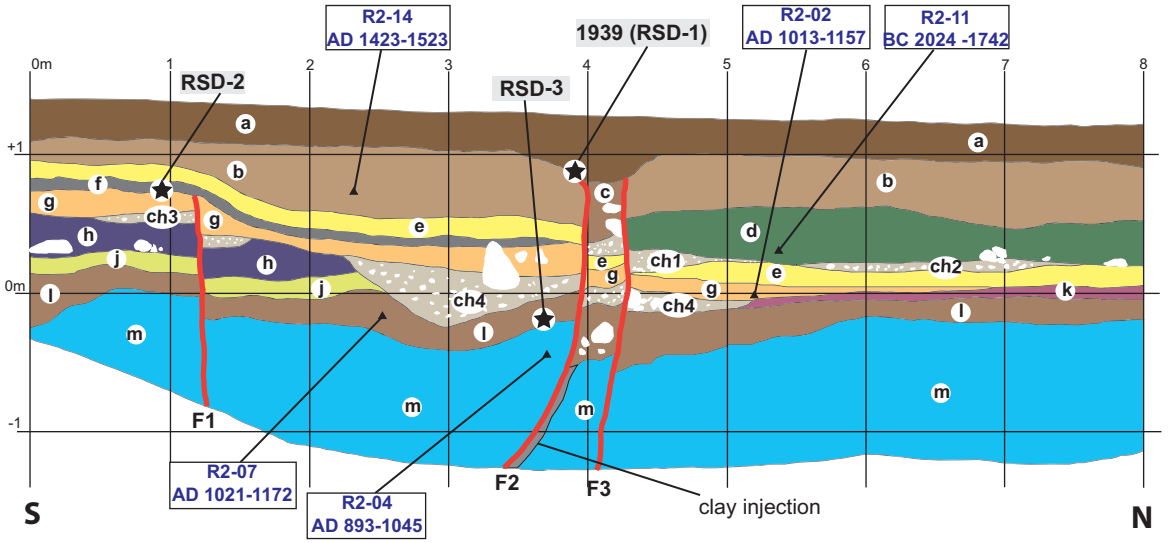

Figure 4. Log of the first 8 metres of the Reşadiye trench (west wall). Stars indicate event horizons, ages of charcoal samples are shown on the log with their highest 2σ probabilities (details in Table 2). Stratigraphy: **a**– ploughed zone, **b**– light brown clay, **c**– cobbles and pebbles in clay matrix (infill of the 1939 event), **d**– greenish brown clay with little amount of caliches content, **e**– yellow silt, **f**– dark grey clay (post-RSD-2 deposits), **g**– fine sand with pebble content, **h**– sand with pebbles and cobbles close to the lower boundary, **j**– coarse sandy silt, **k**– fine sand with pebbles, **l**– brown silt (post RSD-3? deposits), **m**– pebbles, cobbles, and boulders in fine sand-silty matrix, and **ch**– channel deposits.

collected from unit b only one gave a reliable date. Sample R2-14 from the middle-to-lower sections of unit b yielded an age of A.D. 1423–1523 (highest 2σ probability); two samples yielded inconsistent much older ages and the other one contained insufficient carbon for dating. At the lower boundary, there are two independent ages: A.D. 1013–1157 (R2-02) and A.D. 1021–1172 (R2-07), respectively from units g and l (Figure 4). Although the slightly younger date from unit g (sample R2-02) is little problematic with respect to the stratigraphic relationship, it can be suggested that the lower boundary for the RSD-2 event is limited to the 12th century.

The amount of offset at the upper surface of unit m is almost twice that of higher units, such as units l, g, e and ch1 (Figure 4). In addition, a thin clay injection along F2 does not extend further up and ends below unit l (Figure 4). These observations on the trench wall suggest that fault F2 had been previously reactivated, but not during the F1 faulting. This is evidence for a palaeoevent (RSD-3) prior to RSD-2 and we place the event horizon at the base of unit l. Two charcoal samples below (R2-04) and above (R2-07) the event horizon yielded calibrated ages of A.D. 893–1045 and A.D. 1021–1172, respectively. The ages of dated samples suggest that event RSD-3 took place between A.D. 893 and 1172.

Umurca Trench

The Umurca trench was excavated in alluvial fan deposits about 3 km east of Umurca village (UMR site in Figure 2). The site was selected was made following the villagers' confirmation of the 1939 rupture location, the presence of fine distal deposits of the alluvial fan, and the existence of an E–W-elongated ridge at this location. The trench is 15 m long and about 2 m deep, exposing a sequence of predominantly very fine to fine clastic material (clay, silt), with intercalated layers of pebbles and sands. Large blocks, preventing deeper excavation, exist at the base of the trench. A brief description of all stratigraphic units is given in Figure 5. Seven charcoal samples were dated from units d, e, f, g, and h (samples UMR D-1, UMR B-1, UMR B-9, UMR D-2, UMR B-1, and UMR B-7, see Table 2 and Figure 5), although three of the results could not be used in the date determination of palaeoevents due to

the incompatibility of the relative positions of each stratigraphic unit with regard to their absolute ages.

There are many fault branches, terminating at various depths on both walls of the Umurca trench (Figure 5). Fault F2, including sub-parallel branches, extends up to the ploughed zone in both walls and represents the 1939 rupture (UMR-1). There is a clear sheared zone between fault planes on the west wall. Units y, z and w show lateral discontinuity due to the activity of this zone. Units c and i are downthrown up to 30 cm on the south side of the fault (Figure 5).

The penultimate event, UMR-2, is determined at the fifth metre by the truncation of fault F3 below unit e. The faulting is characterized by lateral abrupt discontinuation of all units below unit e, which overlies all offset layers and shows no sign of deformation. Thus, we interpret the basal contact of unit e as an event horizon (UMR-2). A charcoal sample (UMR B-4) from the upper sections of unit g was dated as A.D. 1622–1668 with 53.70% 2σ probability. On the east wall, there is another charcoal sample (UMR D-2), 25 cm below the event horizon (middle section of unit h) of penultimate surface rupture, yielding an age interval of A.D. 1415–1451. Samples UMR B-9 and UMR B-3 are interpreted to be reworked material which gave older ages than samples from stratigraphically older units. The charcoal sample (UMR D-1) above the event horizon of UMR-2 yielded an age younger than 300 years (the highest 2σ probability of this sample is A.D. 1726–1814) but this time interval is problematic, because of the 'radiocarbon plateau' produced by fossil fuel combustion (Suess Effect; Suess 1965) and increasing solar activity following the Maunder minimum (Stuiver & Quay 1980). Based on radiocarbon dating (Table 2), we suggest that event UMR-2 took place after the 17th century, most probably after the mid 1600s and before the end of the 18th century.

Fault F4 terminates below unit h (Figure 5c) and we interpret this south-dipping fault as the result of the pre-penultimate event (UMR-3). On the east wall, fault F4 has a straighter geometry at the sixth metre and is again overlain by unit h. While deformation is expressed by an abrupt change of dip angle of units k, l, m and o on the western wall, it is characterized by; (1) vertical separation, (2) change of layer thicknesses, and (3) lateral discontinuity on the eastern wall. In addition, in the middle part of the trench (between 2nd and 4th metres), several faults (indicated as FZ in Figure 5c) are overlain by unit g. The stratigraphic record suggests that unit g is the last deformed unit by the UMR-2 event. By using the spatial consistency of the event horizon, which overlain by unit g, this event can be correlated with UMR-3. Nevertheless, we prefer to name this event UMR-3? because of the lateral difference of stratigraphic units on both sides of the fault F3, preventing a full correlation, between second-to-fourth and fifth-to-seventh metres of the trench. Sample UMR D-2, from the middle sections of unit h, is dated to A.D. 1415–1451 as the upper limit for the pre-penultimate event (UMR-3). UMR B-7 yields an age of A.D. 430–600 for the lower section of unit k, below the event horizon of the UMR-3 event. An interval between the sixth and fifteenth centuries is too wide to correlate this faulting evidence with any historical earthquake.

The oldest event (UMR-4) is expressed by the upper termination of fault F1 which splayed from the main zone of the 1939 surface rupture between 1 and 2 metres of the Umurca trench's eastern and western walls. Fault F1 bounds units w, z and y in the north and terminates at the contact between units y and i (Figure 5c). Thus, we place the event horizon of UMR-4 below unit i. We could not find any datable material (such as charcoal and/or wood pieces) in unit I because it consists mainly of pebbles, cobbles and, rarely, blocks. A sample from unit y yielded an age of B.C. 2819–2662, but this is probably reworked material. Thus, we could not provide any age constraints for the oldest event in the Umurca trench due to the absence of datable material above or below the event horizon.

Palaeoearthquakes on the Kelkit Valley Segment

We found evidence of 4 palaeoearthquakes, including the 1939 event, in the Reşadiye and Umurca trenches on the basis of sedimentary and structural relations. These results are correlated with other nearby palaeoseismic studies and recorded historical events. The abridged table of historical earthquakes for the region between Niksar and Erzincan is compiled from the earthquake catalogue of Tan *et al.* (2008) (Table 3). Examination of this table showed that most significant events that might have caused surface

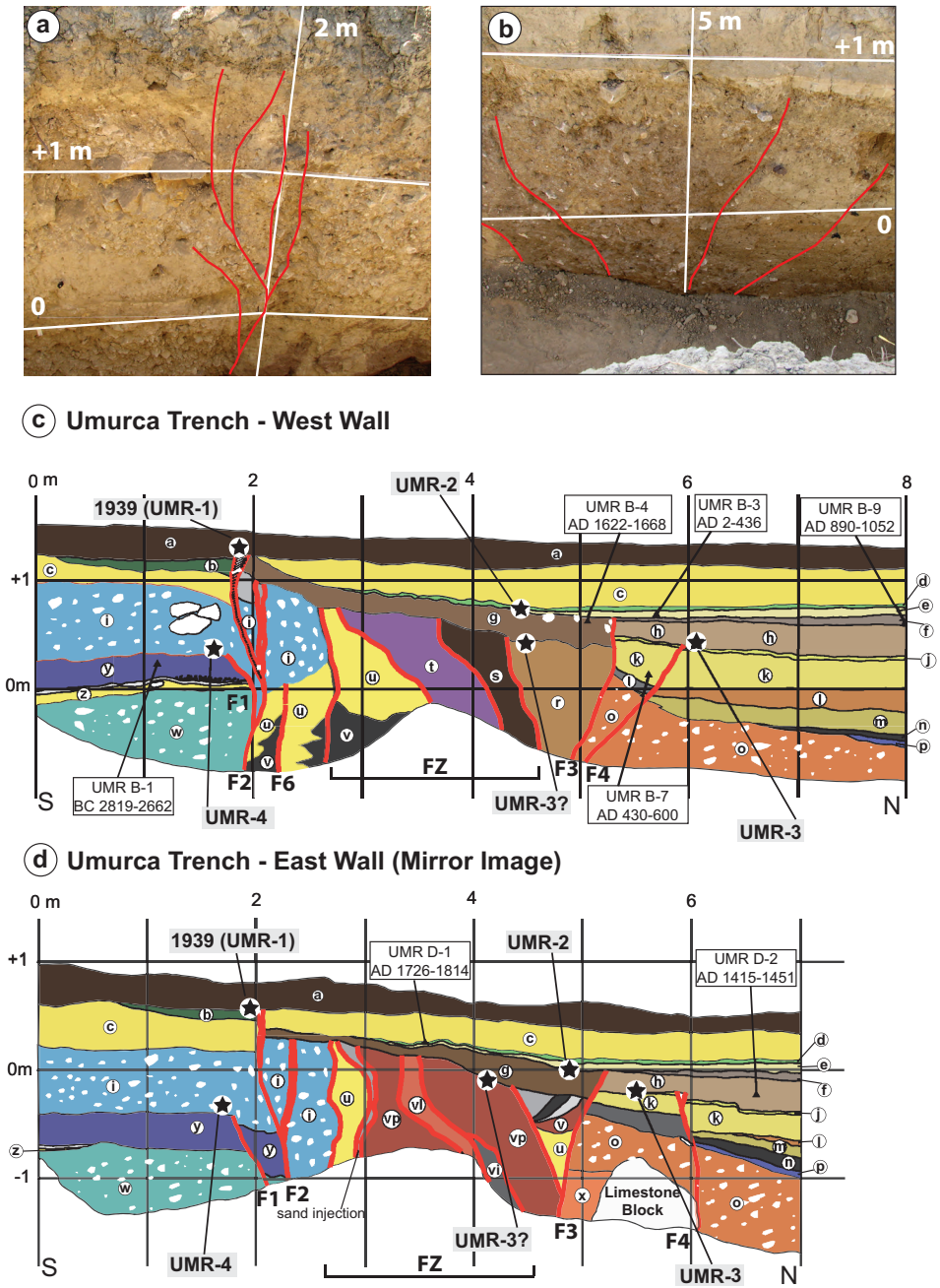

Figure 5. **(a)** Trace of the 1939 earthquake fault on the west wall of the Umurca trench (2nd metre). **(b)** Faulting related to the penultimate and pre-penultimate events on the west wall (between 4th and 6th metres). **(c)** Log of the Umurca trench (west wall). Ages of charcoal samples are shown on both walls with their highest 2σ probabilities. **(d)** Log of eastern wall which reflected over the vertical axis to make an easier visual correlation with the western wall. Stratigraphy for both walls: **a**– ploughed zone (overlain the 1939 event), **b**– greenish brown silt with few gravels, **c**– yellow silt, **d**– sand, **e**– light yellow silt (is the post UMR-2 event deposits), **f**– light brown clay, **g**– brown pebbly silt (is above the event horizon of the UMR-3? event), **h**– brown clayey sand (is the covering unit of UMR-3), **i**– pebbles and cobbles in yellow silt matrix, **j**– sand, **k**– yellow silty clay with pebbles, **l**– light brown clay, **m**– yellow silt, **n**– brownish clay, **o**– brown clay with pebbles and cobbles, **p**– yellow silty clay, **r**– pebbles in yellowish brown clay, **s**– dark brown gravely clay, **t**– pebbles in light yellow silt matrix **u**– yellow silt **v**– red clay, **vi**– yellow clay, **vl**– light red clay with pebbles, **vp**– pebbles in red clay, **w**– pebbles, cobbles, and boulders in yellow silt matrix, **x**– silt with few pebbles, **y**– yellow silty clay with few pebbles, and **z**– yellow silt

Table 3. Recorded historical earthquakes between Niksar and Erzincan (Tan *et al.* 2008). The last column is used for abbreviations for reference. HS– Soysal *et al.* 1981; EG– Guidoboni *et al.*1994; AJ– Abraseys & Jackson 1998; ST– Shebalin & Tatevossian 1997; EG2– Guidoboni & Comastri 2005; KU– Kondorskaya & Ulomov 1999.

Year	Month	Day	Location	Lat	Lon	M	Ref.
127	0	0	Niksar	40.6	37	0	HS
330	0	0	Niksar	40.6	37	0	HS
335	0	0	Niksar	40.6	37	0	HS
343	0	0	Niksar	40.6149	36.9345	6.9	EG
366	0	0	Niksar	40.6	37	0	HS
499	9	0	Niksar?	40.5	37	0	AJ
506	0	0	Niksar	40.6	36.9	0	HS
802	0	0	Erzincan	39.7	39.5	6.5	ST
1011	0	0	Erzincan	39.7	39.5	6.5	ST
1045	0	0	Erzincan	39.7333	39.5	8.1	EG2
1045	4	5	Suşehri?	40	38	0	AJ
1047	0	0	Erzincan	39.75	39.5	0	HS
1068	0	0	Erzincan	39.75	39.5	0	HS
1236	0	0	Erzincan	39.75	39.5	0	HS
1254	4	28	Suşehri	40.2	38.3	7.2	ST
1254	10	11	Erzincan	39.7333	39.5	7.5	EG2
1281	0	0	Erzincan	39.75	39.5	0	HS
1287	5	16	Erzincan	39.7333	39.5	6.9	EG2
1289	0	0	Erzincan	39.75	39.5	0	HS
1290	0	0	Erzincan	39.75	39.5	0	HS
1345	0	0	Erzincan	39.75	39.5	0	HS
1356	0	0	Erzincan	39.75	39.5	0	HS
1366	0	0	Erzincan	39.75	39.5	0	HS
1419	3	26	Erzincan	39.7333	39.5	6.6	EG2
1422	0	0	Erzincan	39.75	39.5	0	HS
1433	0	0	Erzincan	39.75	39.5	0	HS
1456	4	13	Erzincan	39.75	39.5	0	HS
1482	12	21	Erzincan	39.75	39.5	0	HS
1576	11	5	Erzincan	39.75	39.5	0	HS
1583	5	28	Erzincan	39.75	39.5	0	HS
1584	6	17	Refahiye	40	39	6.6	ST
1666	0	13	Erzincan	39.7	39.5	7.5	ST
1668	8	17	Anadolu	41	36	8.1	KU
1787	0	0	Erzincan	39.75	39.5	0	HS
1887	7	0	Tokat	40.3	36.5	0	HS
1888	5	0	Erzincan	39.75	39.5	0	HS
1890	5	20	Refahiye	39.9	38.8	0	HS
1890	0	0	Niksar	40.6	36.9	0	HS

rupture in the Kelkit Valley segment occurred at A.D. 1045, A.D. 1254, A.D. 1666 and A.D. 1668.

Figure 6 summarizes the age ranges of palaeoearthquakes recognized in the trenches and their possible relation to each other. Although evidence for the 1939 surface rupture (RSD-1 and UMR-1) is clear in both the Reşadiye and Umurca trenches, evidence for other events does not represent the same time period. While the penultimate event (RSD-2) in the Reşadiye trench took place between the 12th and 15th centuries, exposed evidence in the Umurca trench suggests that the last event (UMR-2) prior to the 1939 rupture occurred after early 1600s and before the end of the 18th century (between A.D. 1618 and 1778 with 68.2% probability).

We propose two hypotheses to explain this disagreement: (a) the fault section at the Umurca site experienced an additional and younger earthquake during the last 600 years with respect to the Reşadiye part or (b) evidence of a younger event prior to the RSD-2 is missed in the Reşadiye trench either because of the subjectivity component of the observation or the lack of sedimentation/presence of erosion that would record the surface rupture. The first hypothesis is not credible because of the proximity (only 25 km) of the two trenches. But more careful examination of the Reşadiye trench site shows many agricultural fields dominating the area (Figure 3a). There are two main parallel south-flowing drainage patterns. These fields are all on the alluvial fan deposits related to the eastern drainage in the trench area. We noticed an artificial channel, changing the drainage of the eastern stream and connecting it to the western one. This modification is probably made for an irrigation system for all the agricultural fields in the area. Moreover, we measured seven horizontal slips on the boundaries of these fields, with shifts of between 4 and 10.8 metres. The minimum horizontal offset, measured at around 4 m at least in four field boundaries, is the product of the 1939 event. In addition, there are two ~6.5 m offset measurements as a second order set and one of 10.8 m as a third order set of horizontal slip (Figure 3b). We interpret all these different sets of measurements as reflecting multiple events, for which each set represents an individual earthquake. If we assume that there is no time gap between these sets' records, we can calculate the horizontal slip to be around 2.5 m for the penultimate event (UMR-2) and about 4 m for the pre-penultimate rupture (RSD-2 and UMR-3). The modification of the drainage system and preservation of these cumulative offsets suggest a hiatus which is thought to cause the lack of evidence after the 15th century in the Reşadiye trench. While it looks like a disadvantage at the beginning, the preservation of cumulative offsets and including those of prior events at more shallow depths helped us determine these older events and calculate their possible individual horizontal slip. Two large historical earthquakes, A.D. 1666 and A.D. 1668, can be correlated within the age interval of the UMR-2 event. As it is known that the 1666 event affected mainly the Erzincan area and there are no records of damage west of Erzincan (Pınar & Lahn 1952), we suggest the A.D. 1668 earthquake was the penultimate event (UMR-2) in the Umurca trench.

The pre-penultimate event is exposed in both the Reşadiye (RSD-2) and Umurca (UMR-3) trenches. Its upper age is constrained to be before A.D. 1423–1523 in the Reşadiye trench and A.D. 1415–1451 in the Umurca trench. These results suggest that the 15th century is the upper boundary for this surface rupture. Although the Umurca trench does not provide a reliable age for the lower limit of this event, two samples from two independent layers below the event horizon in the Reşadiye trench show that event RSD-2 took place after the 12th century. Modelled dates give an interval for event RSD-2/UMR-3 between A.D. 1201 and 1414 with 68.2% probability (Figure 6). As Table 3 shows, there are many recorded historical events for this age interval in Erzincan. However, either most of them are known to have only affected the city centre of Erzincan and nearby regions or provide no detailed data about the damage distribution. On 11 October 1254, a strong earthquake caused heavy damage in Erzincan. Although no damage was reported, Niksar is also known to be struck by the same event. William of Rubruck, a Franciscan priest who travelled through the region in February 1255, about five months after the earthquake, mentioned continuous surface fissures and cracks at least 50 km west of Erzincan city centre (Guidoboni & Comastri 2005). This event is also interpreted to have a rupture length of 150 km and be associated with large displacements in view

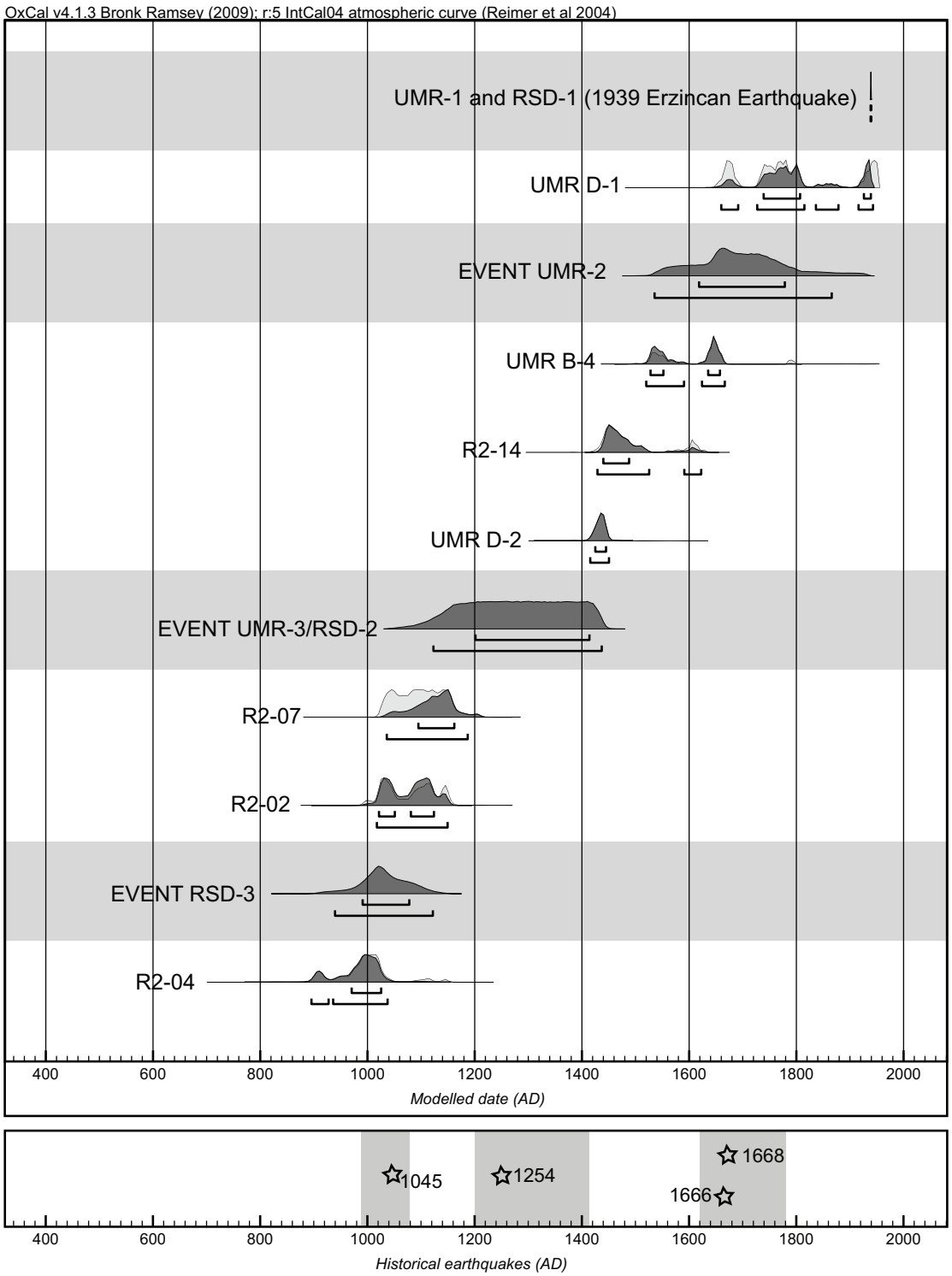

Figure 6. Palaeoearthquakes recognized in the Reşadiye and Umurca trenches and their inferred age ranges. Broader limits, below each age curve; thinner ones represent 95.4% and 68.2% probability, respectively. Events are correlated between trenches on the basis of their age. At the bottom, historical earthquakes (most significant ones from Tan *et al.* 2008, for the region) are shown with stars. Grey boxes in the historical earthquakes section indicate the most probable age intervals (68.2% probability) for each determined event.

of the damage distribution (Ambraseys & Melville 1995). In addition, the 1254 event was suggested as the penultimate event at Çukurçimen, Refahiye in the palaeoseismic study of Hartleb *et al.* (2006). Thus, the A.D. 1254 historical earthquake is a strong candidate for the interval of palaeoseismic results for the RSD-2 and UMR-3 events. Hence, we may say that the surface rupture of the 1254 event extended for a distance of at least 200 km west from Erzincan.

The oldest evidence of faulting with age evaluation, determined in this study, is the RSD-3 event in the Reşadiye trench. The event horizon is limited by the ages A.D. 1021–1172 and A.D. 893–1045 as the upper and lower boundary, respectively. These lower and upper boundary ages are modelled to an interval between A.D. 991 and 1078 with 68.2% probability (Figure 6). According to historical earthquake catalogues (Ergin *et al.* 1967; Ambraseys & Jackson 1998; Guidoboni & Comastri 2005), the A.D.1045 earthquake is known as a large event that almost entirely destroyed Erzincan city. In addition, Hartleb *et al.* (2006) found faulting evidence of the A.D.1045 event in the Çukurçimen trench, Refahiye. We correlated the RSD-3 event with the A.D. 1045 historical earthquake by extrapolating the extent of its surface rupture westwards from Erzincan.

Discussion

Geochronologically constrained age ranges for palaeoearthquakes from the Reşadiye and Umurca trenches are correlated by using historical records with the A.D. 1045, A.D. 1254, and A.D. 1668 historical events prior to the 1939 rupture. Our findings for the A.D. 1045 and A.D. 1254 earthquakes match with palaeoevents in the Çukurçimen (Refahiye) trench (Hartleb *et al.* 2006), about 150 km east of the study area. Palaeoseismic data for the 17 August 1668 Anatolian earthquake are reported in various trench studies conducted on the A.D. 1944, A.D. 1943 and A.D. 1942 earthquake segments of the North Anatolian Fault (Figure 1). It is also known that the western extent of the 1939 rupture did not propagate along the main trace of the North Anatolian Fault around Niksar where there is a 10-km-wide releasing stepover (Figure 1b), which acted as a seismic barrier during this event (Barka & Kadinsky-Cade 1988; Wesnousky 1988, 2006).

Observational studies on earthquake rupture propagation imply that earthquakes can often propagate across small stepovers but are stopped by larger ones (e.g., Wesnousky 1988; Lettis *et al.* 2002; Wesnousky 2006, 2008). Based on worldwide field data of many earthquake ruptures, Knuepfer (1988) suggested a maximum jumpable width of 8 km for dilatational stepovers. Lettis *et al.* (2002) compiled data from 30 historical strike-slip earthquakes including 59 dilatational stepovers and stated that a rupture may not jump dilatational stepovers more than 4–5 km wide. Moreover, in dynamic rupture modelling with homogenous initial fault stress, the largest jumpable width was found to be 5 km for a dilatational stepover (Harris & Day 1993). 3D physical models of spontaneous rupture propagation on strike-slip faults, in an elastic medium, demonstrate that wide stepovers (>5 km) will rarely be jumped during an earthquake (Harris & Day 1999). However, another numerical model, assuming heterogeneous fault stress distribution, shows that a rupture may jump 8 km or wider dilatational stepovers if the fault system has historically experienced many earthquakes (Duan & Oglesby 2006). In other words, a mature fault system tends to allow ruptures to jump wider stepovers than a young fault system, according to this model. The 2001 Kunlunshan, China, earthquake (M_w 7.8), during which the rupture jumped more than 10 km in a releasing stepover, supports this dynamic rupture model with heterogeneous fault stress distribution. Studies, documenting the surface distribution of this very large earthquake, observed a 30 km diagonal gap (Fu *et al.* 2005) or very little surface offset (Xu *et al.* 2006) in this stepover.

The Reşadiye and Umurca trenches are located further east than the 10-km-wide stepover in Niksar (Figure 1b) and they provide evidence for the 1668 earthquake. Hence, we suggest two hypotheses about the surface rupture distribution of the 17 August 1668 Anatolian earthquake: (1) the 1668 event caused a single rupture, probably extending from east of Bolu to Koyulhisar, which also jumped the 10-km-wide releasing stepover in Niksar; (2) there were multiple events between July and September 1668 and several individual rupture zones occurred on different segments of the North Anatolian Fault.

Although numerical models using a homogenous initial fault stress show the maximum jumpable width of dilatational stepovers as 5 km, ruptures can jump more than 8-km-wide releasing stepovers in models with the assumption of a heterogeneous stress fault setting where multi-cycle earthquakes are experienced. Moreover, palaeoseismic studies by Kondo *et al.* (2009) showed an approximate 6 m offset for the 1668 event in Niksar, the eastern end point of the main fault segment before it jumps the 10-km-wide releasing stepover towards the east. In addition, the presence of linking normal faults in the Niksar stepover (Kondo *et al.* 2006) creates a case that is known to greatly increase the ability of earthquake rupture to propagate across a stepover (Oglesby 2005). Thus, we prefer the first hypothesis and suggest that the rupture zone of the 1668 earthquake propagated across the Niksar stepover and terminated somewhere near Koyulhisar. The existence of field boundaries offset by up to 6.5 m (second order set) around Reşadiye (Figure 3b) yields a 2.5 m offset for the 1668 earthquake when considering the 4 m measured offset (Barka 1996) for the 1939 earthquake. This case is similar to the slip distribution of the 2001 Kunlunshan earthquake in which the main eastern segment shows a horizontal offset around 5 metres close to its western tip and an average of 2-to-3 metres further west (Lasserre *et al.* 2005; Xu *et al.* 2006), after the rupture propagated through the releasing stepover.

Conclusions

On the basis of palaeoseismic trenching, we found three palaeoevents (UMR-2, RSD-2/UMR-3, and RSD-3) which are dated and can be correlated to historical events of the A.D. 1668, 1254 and 1045 prior to the 1939 Erzincan earthquake. Evidence of the 17 August 1668 Anatolia earthquake is reported in many palaeoseismological studies performed on the 1944, 1943 and 1942 earthquake ruptures of the North Anatolian Fault. We suggest that the surface rupture of the 1668 earthquake jumped the 10-km-wide releasing stepover in Niksar and continued eastwards to near Koyulhisar. The existence of different amount of cumulative offset in field boundaries (sets of 4 m, 6.5 m and 10.8 m) in the Reşadiye site is the result of multiple events in which the 1939, 1668 and 1254 surface ruptures have about 4, 2.5 and 4 metres of coseismic horizontal slip, respectively.

Acknowledgements

This work was supported by T.C. D.P.T. Project No. 2006K120220. We wish to thank all local authorities for their help, land owners for giving us permission to excavate their lands, and Mr. Rüstem Yıldız for useful guidance in the field at the location of the 1939 rupture. The first two figures were drawn using Generic Mapping Tools (Wessel & Smith 1998). We are indebted to Özgür Kozacı and Hasan Sözbilir for reviews that substantially improved the paper.

References

Akyüz, H.S., Hartleb, R., Barka, A.A., Altunel, E. & Sunal, G. 2002. Surface rupture and slip distribution of the 12 November 1999 Düzce Earthquake (M 7.1), North Anatolian Fault, Bolu, Turkey. *Bulletin of the Seismological Society of America* **92**, 61–66.

Ambraseys, N.N. & Finkel, C.F. 1988. The Anatolian Earthquake of 17 August 1668. *In*: Lee, W.H.K., Meyers, H. & Shimazaki, K. (eds), *Historical Seismograms and Earthquakes of the World*. Academic Press, San Diego, 173–180.

Ambraseys, N.N. & Jackson, J.A. 1998. Faulting associated with historical and recent earthquakes in the Eastern Mediterranean region. *Geophysical Journal International* **133**, 390–406.

Ambraseys, N.N. & Melville, C.P. 1995. Historical evidence of faulting in Eastern Anatolia and Northern Syria. *Annali Di Geofisica* **XXXVIII**, 337–343.

Ambraseys, N.N. & Zatopek, A. 1969. The Mudurnu valley, west Anatolia, Turkey, earthquake of 22 July 1967. *Bulletin of the Seismological Society of America* **59**, 521–589.

Barka, A.A. 1992. The North Anatolian fault zone. *Annales Tectonicae* **6**, 164–195.

Barka, A.A. 1996. Slip distribution along the North Anatolian Fault associated with large earthquakes of the period 1939 to 1967. *Bulletin of the Seismological Society of America* **86**, 1238–1254.

Barka, A.A. 1999. The 17 August 1999 İzmit Earthquake. *Science* **285**, 1858–1859.

Barka, A.A., Akyüz, H.S., Altunel, E., Sunal, G. & Çakir, Z. 2002. The surface rupture and slip distribution of the 17 August 1999 İzmit earthquake (M 7.4), North Anatolian Fault. *Bulletin of the Seismological Society of America* **92**, 43–60.

Barka, A.A., Akyüz, H.S., Cohen, H.A. & Watchorn, F. 2000. Tectonic evolution of the Niksar and Taşova-Erbaa pull-apart basins, North Anatolian Fault Zone: their significance for the motion of the Anatolian block. *Tectonophysics* **322**, 243–264.

Barka, A.A. & Kadinsky-Cade, K. 1988. Strike-slip fault geometry in Turkey and its influence on earthquake activity. *Tectonics* **7**, 663–684.

Blumenthal, M.M. 1945. Ladik deprem hattı (Samsun ili); la ligne sismique de Ladik, Vilayet de Samsun. *Maden Tetkik ve Arama (MTA) Dergisi* **33**, 153–174.

Bronk Ramsey, C. 2009. Bayesian analysis of radiocarbon ages. *Radiocarbon* **51**, 337–360.

Dewey, J.W. 1976. Seismicity of Northern Anatolia. *Bulletin of the Seismological Society of America* **66**, 843–868.

Duan, B. & Oglesby, D.D. 2006. Heterogeneous fault stresses from previous earthquakes and the effect on dynamics of parallel strike-slip faults. Journal of Geophysical Research 111, 1-15.

Ergin, K., Güçlü, U. & Uz, Z. 1967. *Türkiye ve Civarının Deprem Kataloğu (Milattan Sonra 11 yılından 1964 Sonuna Kadar) [Earthquake Cataloque of Turkey and Nearby Regions (From A.D. 11 to 1964)]*. İTÜ Maden Fakültesi Ofset Matbaası, İstanbul.

Fraser, J., Pigati, J.S., Hubert-Ferrari, A., Vanneste, K., Avşar, U. & Altinok, S. 2009. A 3000-year record of ground-rupturing earthquakes along the Central North Anatolian Fault near Lake Ladik, Turkey. *Bulletin of the Seismological Society of America* **99**, 2681–2703.

Fu, B., Awata, Y., Du, J., Ninomiya, Y. & He, W. 2005. Complex geometry and segmentation of the surface rupture associated with the 14 November 2001 great Kunlun earthquake, northern Tibet, China. *Tectonophysics* **407**, 43–63.

Guidoboni, E. & Comastri, A. 2005. *Catalogues of Earthquakes and Tsunamis in the Mediterranean Area from the 11th to 15th Century*. Istituto Nazionale di Geofisica e Vulcanologia, Rome.

Guidoboni, E., Comastri, A. & Traina, G., 1994. *Catalogue of Ancient Earthquakes in the Medditerranean Area up to the 10th Century*. INGV, Roma.

Harris, R. & Day, S. 1993. Dynamics of fault interaction: parallel strike-slip faults. *Journal of Geophysical Research* **98**, 4461–4472.

Harris, R. & Day, S. 1999. Dynamic 3D simulations of earthquakes on en echelon faults. *Geophysical Research Letters* **26**, 2089–2092.

Hartleb, R.D., Dolan, J.F., Akyüz, H.S. & Yerli, B. 2003. A 2000-year-long paleoseismologic record of earthquakes along the central North Anatolian Fault, from trenches at Alayurt, Turkey. *Bulletin of the Seismological Society of America* **93**, 1935–1954.

Hartleb, R.D., Dolan, J.F., Kozaci, Ö., Akyüz, H.S. & Seitz, G.G. 2006. A 2500-yr-long paleoseismologic record of large, infrequent earthquakes on the North Anatolian fault at Çukurçimen, Turkey. *Geological Society of America Bulletin* **118**, 823–840.

Ketin, İ. 1948. Ueber die tektonisch-mechanischen Folgerungen aus den grossen anatolischen Erdbeben des letzten Dezenniums. *Geologische Rundschau* **36**, 77–83.

Ketin, İ. 1969. Kuzey Anadolu Fayı hakkında [About the North Anatolian Fault]. *Maden Tetkik ve Arama Dergisi* **72**, 1–27 [in Turksih].

Knuepfer, P.L.K. 1988. Implications of the characteristics of end-points of historical surface fault ruptures for the nature of fault segmentation. *In*: Schwartz, D.P. & Sibson, R.H. (eds) *Fault Segmentation and Controls of Rupture Initiation and Termination*. U.S. Geological Survey, 193–228.

Kondo, H., Awata, Y., Emre, Ö., Doğan, A., Özalp, S., Tokay, F., Yildirim, C., Yoshioka, T. & Okumura, K. 2005. Slip distribution, fault geometry, and fault segmentation of the 1944 Bolu-Gerede earthquake rupture, North Anatolian Fault, Turkey. *Bulletin of the Seismological Society of America* **95**, 1234–1249.

Kondo, H., Emre, Ö. & Yildirim, C. 2006. Surface ruptures associated with the 1942 and 1951 earthquakes along the North Anatolian fault system – implications for non-characteristic earthquakes and macroscopic barrier segments. *EGU, Geophysical Research Abstracts*, *Vienna*. 8, 02473.

Kondo, H., Kürçer, A., Özalp, S. & Emre, Ö. 2009. Non-characteristic recurrence behavior on the 1942 Niksar-Erbaa earthquake rupture along the North Anatolian fault system, Turkey. *EGU General Assembly – Geophysical Research Abstracts*, *Vienna*. 11, EGU2009-7712-2.

Kondo, H., Özaksoy, V. & Yildirim, C. 2010. Slip history of the 1944 Bolu-Gerede earthquake rupture along the North Anatolian Fault System: implications for recurrence behavior of multisegment earthquakes. *Journal of Geophysical Research* **115**, 1–16.

Kondo, H., Özaksoy, V., Yildirim, C., Awata, Y., Emre, Ö. & Okumura, K. 2004. 3D trenching survey at Demir Tepe site on the 1944 earthquake rupture, North Anatolian Fault System, Turkey. *Annual Report on Active Fault and Paleoearthquake Researches*, 231–242.

Kondorskaya, N.V. & Ulomov, V.I. 1999. Special Catalogue of Earthquakes of the Northern Eurasia (SECNE). *http://www.seismo.ethz.ch/gshap/neurasia/nordasiacat.txt*, Access date: 25.01.2009

Kurçer, A., Kondo, H., Özalp, S. & Emre, Ö. 2009. Paleoseismological findings on the western portion of the surface rupture associated with 1942 Erbaa-Niksar earthquake, North Anatolian faut system, Turkey. *EGU General Assembly - Geophysical Research Abstracts*, *Vienna* 11, EGU2009-8733.

Lasserre, C., Peltzer, G., Crampe, F., Klinger, Y., Woerd, J.V.D. & Tapponnier, P. 2005. Coseismic deformation of the 2001 Mw= 7.8 Kokoxili earthquake in Tibet, measured by synthetic aperture radar interferometry. *Journal of Geophysical Research* **110**, 1–17.

Lettis, W., Bachhuber, J., Witter, R., Brankman, C., Randolph, C.E., Barka, A.A., Page, W.D. & Kaya, A. 2002. Influence of releasing step-overs on surface fault rupture and fault segmentation: examples from the 17 August 1999 İzmit earthquake on the North Anatolian Fault, Turkey. *Bulletin of the Seismological Society of America* **92**, 19–42.

McKenzie, D. 1972. Active tectonic of the Mediterranean region. *The Geophysical Journal of the Royal Astronomical Society* **30**, 109–185.

Oglesby, D.D. 2005. The dynamics of strike-slip step-overs with linking dip-slip faults. *Bulletin of the Seismological Society of America* **95**, 1604–1622.

Okumura, K., Rockwell, T.K., Duman, T., Tokay, F., Kondo, H., Yildirim, C. & Özaksoy, V. 2003. Refined slip history of the North Anatolian Fault at Gerede on the 1944 rupture. *EOS Transacations, AGU*, *San Francisco*. 84, S12B-0384.

Parejas, E., Akyol, I.H. & Altinli, E. 1942. 27 Aralık 1939 Erzincan yerdepremi (batı kısmı); la tremblement de terre d'Erzincan du 27 decembre 1939 (secteur occidentale). *İstanbul University, Institute of Geology, Publications* **B6***(Nos. 3-4);* **10**, 187–222.

Pinar, N. & Lahn, E. 1952. *Türkiye Depremleri İzahlı Kataloğu [Earthquake Cataloque of Turkey with Explanations]*. TC Bayındırlık Bakanlığı Yapı ve İmar İşleri Reisliği Yayınları, Ankara.

Pucci, S., Palyvos, N., Zabci, C., Pantosti, D. & Barchi, M. 2006. Coseismic ruptures and tectonic landforms along the Düzce segment of the North Anatolian Fault Zone (Ms 7.1, November 1999). *Journal of Geophysical Research* **111**, B06312–B06312.

Reimer, P.J., Baillie, M.G.L., Bard, E., Bayliss, A., Beck, J.W., Bertrand, C.J.H., Blackwell, P.G., Buck, C.E., Burr, G.S., Cutler, K.B., Damon, P.E., Edwards, R.L., Fairbanks, R.G., Friedrich, M., Ramsey, C.B., Reiemer, R.W., Remmele, S., Southon, J.R., Stuvier, M., Talamo, S., Taylor, F.W., van der Plicht, J. & Weyhenmeyer, C.E. 2004. IntCal04 Terrestrial radiocarbon age calibration, 26-0 ka BP. *Radiocarbon* **46**, 1029–1058.

Şaroğlu, F., Emre, Ö. & Kuşçu, İ. 1992. *Türkiye Aktif Fay Haritası [Active Fault Map of Turkey]*. Maden Tetkik ve Araştırma Enstitüsü (M.T.A.).

Şengör, A.M.C. 1979. The North Anatolian transform fault; its age, offset and tectonic significance. *Journal of the Geological Society, London* **136,** 269–282.

Şengör, A.M.C., Tüysüz, O., İmren, C., Sakinç, M., Eyidoğan, H., Görür, N., Le Pichon, X. & Rangin, C. 2005. The North Anatolian Fault: a new look. *Annual Review of Earth and Planetary Sciences* **33**, 37–112.

Seymen, İ. 1975. *Kelkit Vadisi Kesiminde Kuzey Anadolu Fay Zonunun Tektonik Özellikleri [Tectonic Characteristics of the North Anatolian Fault Zone in the Kelkit Valley]*. PhD Thesis, İstanbul Teknik Üniversitesi, İstanbul [in Turkish with English abstract].

Shebalin, N.V. & Tatevossian, R.E. 1997. Catalogue of large historical earthquakes of the Caucasus. *In*: Giardini, D. & Balassanian, S. (eds), *Catalogue of Large Historical Earthquakes of the Caucasus*. Kluwer Academic Publishers, Dordrecht, 201–232.

Soysal, H., Sipahioğlu, S., Kolçak, D. & Altinok, Y. 1981. *Türkiye ve Çevresinin Tarihsel Deprem Kataloğu, MÖ. 2100 - MS. 1900 [Historical Earthquake Cataloque of Turkey and Its Surroundings, BC. 2100–AD. 1900]*. TÜBİTAK Proje No TBAG-341, İstanbul [in Turkish].

Stuiver, M. & Quay, P.D. 1980. Changes in atmospheric Carbon-14 attributed to a variable sun. *Science* **207**, 11–19.

Suess, H.E. 1965. Secular variations of the cosmic-ray-produced Carbon 14 in the atmosphere and their interpretations. *Journal of Geophysical Research* **70**, 5937–5952.

Sugai, T., Emre, Ö., Duman, T. Y., Yoshioka, T. & Kuşçu, İ. 1999. Geologic evidence for five large earthquakes on the North Anatolian Fault at Ilgaz, during the last 2000 years; a result of GSJ-MTA international cooperative research. *In*: Satake, K. & Schwartz, D.P. (eds), *The Peleoseismology Workshop*. USGS Open-File Report, 66-72.

Tan, O., Tapirdamaz, M.C. & Yoruk, A. 2008. The earthquake catalogues for Turkey. *Turkish Journal of Earth Sciences* **17**, 405–418.

Wesnousky, S.G. 1988. Seismological and structural evolution of strike-slip faults. *Nature* **335**, 340–343.

Wesnousky, S.G. 2006. Predicting the endpoints of earthquake ruptures. *Nature* **444**, 358–360.

Wesnousky, S.G. 2008. Displacement and geometrical characteristics of earthquake surface ruptures: issues and implications for seismic-hazard analysis and the process of earthquake rupture. *Bulletin of the Seismological Society of America* **98**, 1609–1632.

Wessel, P. & Smith, W.H.F. 1998. New, improved version of the Generic Mapping Tools released. *EUS* **79**, 579.

Xu, X., Yu, G., Klinger, Y., Tapponnier, P. & Woerd, J.V.D. 2006. Reevaluation of surface rupture parameters and faulting segmentation of the 2001 Kunlunshan earthquake (Mw 7.8), northern Tibetan Plateau, China. *Journal of Geophysical Research* **111**, 1–16.

Yoshioka, T., Okumura, K., Kuşçu, İ. & Emre, Ö. 2000. Recent surface faulting of the North Anatolian Fault along the 1943 Ladik earthquake ruptures. *Bulletin of the Geological Survey of Japan* **51**, 29–35.